VOL. 14, NO. 20, OCTOBER 2019 ISSN 1819-6608
ARPN Journal of Engineering and Applied Sciences

www.arpnjournals.com

MHD SQUEEZING FLOW OF NANOLIQUID ON A POROUS STRETCHED SURFACE: NUMERICAL STUDY

Mohammed M. Fayyadh[1], R. Roslan[1], R. Kandasamy[2] and Inas R. Ali[1]
[1]RCCFD, Faculty of Applied Sciences and Technology, University Tun Hussein Onn Malaysia, Johor, Malaysia
[2]Knowledge Institute of Technology India, Kalapalayan, Tamil Nadu, India
E-Mail: abuzeen@gmail.com

ABSTRACT

This work is aimed at conducting a comparative study between two base fluids water as well as ethylene glycol along with nanoparticle (oxide aluminium). Analysis is done for determining unsteadiness between two parallel walls, wherein squeezing of upper wall towards lower is done, while porous stretching surface is lower. The mathematical formulation uses constitutive expression pertaining to viscous nanoliquids. By keeping a variable magnetic field, conduction of nanoliquid is done electrically. The partial differential equations concerning the issue were resolved after transforming to ordinary differential equations by employing forth-fifth Runge-Kutta Fehlberg method. The effect of disparity in various parameters pertaining to temperature, velocity and concentration profile of nanoparticle is first plotted and then tabulated. Based on the obtained results, the velocity field was seen to enhance with rise in squeezing parameter values. Squeezing parameters that possess larger values result in decrease in temperature and concentration profiles of nanoparticles. The heat transfer of nanoliquids was seen to improve with squeezing flow, magnetic field parameter and nanoparticle volume fraction. For the rate of skin friction pertaining to ethylene glycol and water, dominance was seen for magnetic parameter M, suction parameter S and nanoparticle volume fraction parameter.

Keywords: nanoliquid, squeezed flow; magnetic field; heat and mass transfer; water and ethylene glycol; numerical analysis.

1. INTRODUCTION

Due to increase in energy prices, improving heat transfer for different energy systems has become very crucial. In the last few years, much interest has been put on convective heat transfer via nanoliquids. The base fluids such as oil, water and ethylene glycol are employed in various industrial processes like in chemical processes, power generation and cooling or heating processes, wherein poor heat transfer fluid displays poor heat transfer characteristics along with low thermal conductivity. This can be enhanced with suspension of solid nanoparticle into the base fluid to raise the thermal conductivity. The poor heat transfer characteristics pertaining to the base fluids were the major hindrance to high compactness as well as heat exchangers' effectiveness (Zaimi, Ishak and Pop, 2014).

Chol and Estman (1995) can be credited to being the first to term the mixture as nanoliquid, wherein base fluids were mixed with solid nanoparticle. Nanoliquids have been reported to possess good stability as well as rheological properties, considerably higher thermal conductivities as well as no penalty pertaining to pressure drop.

Typically, a higher thermal conductivity is associated with solids versus liquids. For instance, a thermal conductivity is associated with copper (Cu), which is 3,000 times greater versus engine oiland 700 times greater versus water. Employing solid particles for the base fluid in the size range of 10-100 nm is considered to be an innovative and novel technique to improve heat transfer (Sheikholeslami, Abelman and Ganji, 2014).

For a majority of issues associated with engineering, particularly for few of the heat transfer equations that are nonlinear, a numerical solution is employed to solve some of these, while for few, a different analytic method like perturbation method is used (Sheikholeslami and Ganji, 2013).

To control heat transfer in a process, few of the researchers put forward nanoliquids technology and studied numericallyor experimentally. Most researchers have presumed nanoliquids to be treated as a common pure fluid as well as employing of conventional equations of momentum, mass and energy, while the only impact of nanoliquid was its viscosity as well as thermal conductivity, which were derived from the experimental data or theoretical models.

A key research topic is evaluating heat and mass transfer pertaining to unsteady squeezing viscous flow between two parallel plates because of its broad range of scientific and engineering applications, like polymer processing, hydro-dynamical machines, food processing, lubrication system, formation and dispersion of fog, chemical processing equipment, damage of crops because of freezing and cooling towers(Sheikholeslami, Ganji and Ashorynejad, 2013).

Idrees *et al.* (2010) investigated the axisymmetric flow pertaining to two-dimensional incompressible fluids by employing the Optimal Homotopy Asymptotic Method (OHAM). The same issue can also be solved with the help of the Homotopy Perturbation Method (HPM), the Perturbation Method (PM) and the Homotopy Analysis Method (HAM). They found OHAM to be parameter free and at lower order of approximation,it gave enhanced accuracy. A squeeze flow was considered by Fang, Gilbert and Liu (2010) between two parallel plates. They employed a partial wall slip to treat both power-law fluid and Newtonian fluid. First a system of equations was derived by employing the lubrication theory approximation for a thin mould, pertaining to a non-isothermal, power-law fluid.

In the nanoliquid model, the important impacts of Brownian motion as well as thermophoresis were considered. Evaluation of two phase simulation pertaining to nanoliquid flow as well as heat transfer between parallel plates was done and the homotopy perturbation method was employed by Sheikholeslami, Hatami and Domairry (2015) to solve the governing equations.

Hayat, Yousaf, *et al.* (2012) evaluated the unsteady two-dimensional flow pertaining to a second-grade fluid between parallel disks exposed to an applied magnetic field. The impact of Newtonian heating on the non-similar mixed convection Falkner–Skan flow was evaluated pertaining to the Maxwell fluid. Hayat, Farooq, *et al.* (2012) performed an analysis by using the Homotopic approach for a series solutions pertaining to temperature and velocity.

By employing the fourth order Runge-Kutta numerical methods well as Homotopy Analysis Method (HAM), Hatami, Nouri and Ganji (2013) evaluated the forced-convection boundary-layer pertaining to MHD Al_2O_3–water nanoliquid flow in a horizontal stretching flat plate.

Loganathan, Nirmal Chand and Ganesan (2013) investigated the impacts of radiation heat transfer on an unsteady natural convective flow pertaining to a nanoliquid. The nanoliquid that included nanoparticles of aluminium oxide, titanium oxide, copper and silver along with its volume was considered. Laplace transform technique fraction was employed to solve the partial differential equations controlling the flow.

The homotopic perturbation method was employed to analytically evaluate heat transfer pertaining to a nanoliquid flow that has been squeezed between parallel plates.

Here, copper has been considered as a nanoparticle where water is the base fluid. Sheikholeslami and Ganji (2013) calculated the effective thermal conductivity as well as viscosity pertaining to nanoliquid.

Sheikholeslami, Abelman and Ganji (2014) studied the nanoliquid flow as well as heat transfer properties pertaining to two horizontal parallel plates in a rotating system. In this model, the impact cast by Brownian motion on the effective thermal conductivity was accounted. The fourth-order Runge–Kutta method was employed to solve these numerically.

A two-dimensional problem was considered by Petrov and Kharlamova (2014) for determining viscous squeezing flow between two parallel plates. The study's goal was velocity profile determination between the plates. Precise solutions pertaining to Navier–Stokes equations were developed as series in powers of Reynolds number.
Khan, Ahmed, Zaidi, *et al.* (2014) investigated via the Variation of Parameters Method, which is an analytical technique, to resolve the squeezing flow issue pertaining to axisymmetric and two-dimensional flows. The computational efficiency of VPM was determined via convergence analysis.

A discussion on magneto hydrodynamic (MHD) squeezing flow pertaining to a viscous fluid has been provided. The Variation of Parameters Method was employed to measure the analytical solution pertaining to the resulting differential equation. The same problem is solved by employing the Runge-Kutta order-4 method in a bid to make a comparison (Khan, Ahmed, Khan, *et al.*, 2014).

Cu-water nanoliquid flow analysis was conducted by Domairry and Hatami (2014) for the two parallel palates by employing the numerical method and a differential transformation method. Padé approximation is used to improve the DTM's accuracy.

The Duan-Rach Approach was employed by Dib, Haiahem and Bou-Said (2015) to get a purely approximate analytical solution pertaining to the squeezing unsteady nanoliquid flow. With the help of the Duan-Rach Approach, an analytical solution can be found out easily without using the numerical methods.

Predictor homotopy analysis method (PHAM) is a new analytical technique to solve the issue of two-dimensional nanoliquid flow by contraction or expansion or of the gaps with permeable walls. The shooting method along with a Runge–Kutta integration method is employed to make a comparison for the PHAM results along with the obtained numerical results. Water is the fluid in the channel that has various nanoparticles: copper, silver, titanium oxide, copper oxide and aluminium oxide as evaluated by Freidoonimehr, Rostami and Rashidi (2015).

Gul *et al.* (2015) evaluated the heat transfer pertaining to the magneto-hydrodynamic (MHD) mixed convection flow of ferro-fluid. As a conventional base fluid, water was used along with nanoparticles of magnetite (Fe_3O_4). Moreover, employing of non-magnetic (Al_2O_3) aluminium oxide nanoparticles was also done. Gupta and Ray (2015) proposed a new method with regards to the Chebyshev wavelet expansion to solve a coupled system that includes nonlinear ordinary differential equations for modelling the unsteady flow showcasing nanoliquid squeezing for the two parallel plates.

Two phase simulation was investigated by Sheikholeslami, Hatami and Domairry (2015) for nanoliquid flow as well as heat transfer between the parallel plates. The key impacts of Brownian motion as well as thermophoresis were accounted for the nanoliquid model. The homotopy perturbation method was employed to solve the governing equations. Freidoonimehr *et al.* (2017) developed a mathematical formulation to study the issue pertaining to heat and mass transfer for MHD Oldroyd-B nanoliquid flow in a stretching sheet when exposed to convective boundary conditions.

A numerical study was performed evaluating the unsteady three-dimensional squeezing flow as well as heat transfer pertaining to an electrically conducting nanoliquid in a rotating channel when there was internal heat source/sink. Four types of nanoparticles were accounted, where water was the base fluid as evaluated by Mahanthesh, Gireesha and Gorla (2016).

Magneto-hydrodynamic (MHD) squeezing flow was considered pertaining to the couple stress nanomaterial between the two parallel surfaces. In the problem formulation, employing of constitutive relations

was done pertaining to couple stress fluid. Novel features associated with Brownian motion and thermophoresis were accounted. Couple stress fluid was conducted electrically that was based on time-dependent applied magnetic field (Hayat, Sajjad, *et al.*, 2017). Dogonchi, Alizadeh and Ganji (2017) investigate the flow and heat transfer properties of MHD Go-water nanoliquid for the two parallel flat plates by exposing to thermal radiation. The Duan–Rach approach was employed to solve the non-linear ordinary differential equations. With the help of this method, the standard Adomian Decomposition Method can be modified by directly assessing the inverse operators along with the boundary conditions.

Hayat, Khan, *et al.* (2017) evaluated the unsteady squeezing flow pertaining to the non-Newtonian nanoliquid for the two parallel plates. A rheological relation describing the second grade liquid was employed. Retention of the Brownian motion, thermal radiation and thermophoresis diffusion was done. Electrical conduction is applied to the second grade liquid in the presence of time-dependent magnetic field. Madaki *et al.* (2018) analytically evaluated the squeezing unsteady nanoliquid flow pertaining to the two parallel plates. The impact of thermal radiation as well as heat absorption/generation along the temperature profile could be seen.

Muhammad *et al.* (2017) evaluated the time-dependent squeezing flow between two parallel wallsfor the magneto-hydrodynamic (MHD) Jeffrey fluid. Stretching of the lower wall is done. By exposing to a variable magnetic field, electrical conduction was done for the fluid. Unsteady flow between two sheets was investigated by Salman Ahmad *et al.* (2018) by considering applied magnetic field, thermal radiation, Joule heating effects and viscous dissipation. Assessment of the entropy generation is also done. The key aim was to make a comparative study for the five water base nanoliquids. A numerical technique for solving was the ordinary differential equations system. S Ahmad *et al.* (2018)investigated the flow characteristics by employing dual stratification. For flowing fluid that includes heat and mass transport, the transport phenomenon was seen to be impacted by the radiative heat flux and the first order chemical reaction. The systems pertaining to non-linear governing equations were seen to be modulating, which was solved by employing the convergent approach (Homotopy Analysis Method).

Ghadikolaei, Hosseinzadeh and Ganji (2018) evaluated three dimensional squeezing flows as well as heat transfer pertaining to (Fe_3O_4)–Ag/ ethylene glycol-water hybrid nanoparticles that were inside a rotating channel along with the fixed and impermeable bottom walls when exposed to thermal radiation.

The heat and mass transfer analysis was discussed based on a novel, multiscale and precise method pertaining to the unsteady nanoliquid flow that has been squeezed between the two parallel plates. The simulations that were seen with the new multiscale scheme were in agreement with the fourth order Runge-Kutta method, which could be extended further to solve other engineering problems that are highly nonlinear (Seyedi, Saray and Ramazani, 2018).

Sheikholeslami *et al.* (2018) studied the impact of magnetic forces on Al_2O_3–H_2O convective flow via a permeable system as shown with the Darcy model. The impacts of Brownian motion as well as particle shapes on nanoliquid behaviour were also considered. Usman *et al.* (2018) investigated the heat transfer as well as flow of water-based copper (Cu) nanoparticles and ethylene glycol between both squeezed parallel disks along with suction/injection impacts. Sobamowo, Jayesimi and Waheed (2018) employed the variation of parameter methodto evaluate the two-dimensional squeezing flow pertaining to the nanoliquid under the influence of the uniform transverse magnetic field as well as slip boundary conditions.

The key aim here is to evaluate the magneto-hydrodynamic (MHD) squeezing flow along with heat as well as mass transfer pertaining to viscous base fluids (ethylene glycol and water) when nanoparticle (Al_2O_3) was used. A movement of the upper impermeable wall towards the lower wall was seen in a time-dependent speed. The lower wall is characterised as being permeable and stretched. Also, the effects of squeezed flow, magnetic field, suction, Brownian motion, Lewis number, nanoparticle volume fraction and thermophoresis parameters have been evaluated. The Runge-Kutta Fehlberg technique was employed to solve the governing nonlinear system.

2. SIMILARITY TRANSFORMATION APPROACH AND GOVERNING EQUATION

This research examines the unstable 2D magneto-hydrodynamic squeezing flow of a viscous that is incompressible along with transfer of heat of nanoliquids ethylene glycol and water as the basic fluids and oxide aluminium as the nanoparticle, and evaluates between a couple of parallel plates that are separated by$\sqrt{\nu(1-\gamma t)/a}$. The plate situated in the upper part at distance $y = h(t) = \sqrt{\nu(1-\gamma t)/a}$ is movable having velocity $-\frac{\gamma}{2}\sqrt{\nu_f/a(1-\gamma t)}$ whereas the porous plate situated in the lower portion at $y = 0$ can be stretched at a velocity of $ax/(1-\gamma t)\,(t < 1/\gamma)$. Observe that the steady state occurrence of linear stretching is regained when $\gamma = 0$. The given fluid is conducting electrically when a magnetic field $B_o/(1-\gamma t)$ is applied in the y–direction (T Hayat *et al.*, 2016). Moreover, the electric fields as well as the Hall effects are disregarded. The magnetic field that is induced is not taken into account in case of a small amount of magnetic Reynolds number. Brownian motion and Thermophoresis effects are preserved. All of the thermo-physical attributes are invariable. The system of coordinates and the flow organisation are displayed in Figure-1.

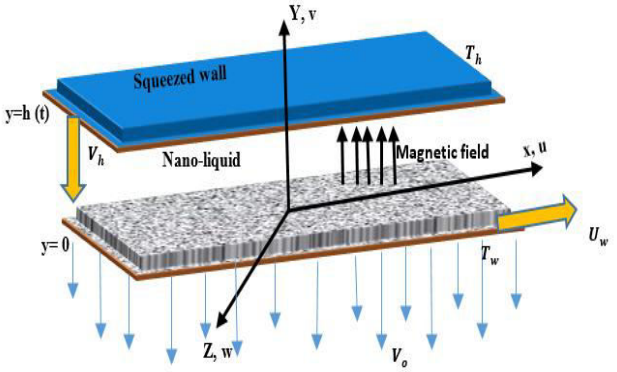

Figure-1. Geometry of the problem.

Allowing for the assumptions and criteria, the PDEs (partial differential equations) which are used to solve this problem are given below:

$$\frac{\partial u}{\partial x}+\frac{\partial v}{\partial y}=0 \quad (1)$$

$$\frac{\partial u}{\partial t}+u\frac{\partial u}{\partial x}+v\frac{\partial u}{\partial y}=-\frac{1}{\rho_{nf}}\frac{\partial p^*}{\partial x}+\nu_{nf}\left(\frac{\partial^2 u}{\partial x^2}+\frac{\partial^2 u}{\partial y^2}\right)-\frac{\sigma_{nf}B_o^2}{\rho_{nf}(1-\gamma t)}u \quad (2)$$

$$\frac{\partial v}{\partial t}+u\frac{\partial v}{\partial x}+v\frac{\partial v}{\partial y}=-\frac{1}{\rho_{nf}}\frac{\partial p^*}{\partial y}+\nu_{nf}\left(\frac{\partial^2 v}{\partial x^2}+\frac{\partial^2 v}{\partial y^2}\right) \quad (3)$$

$$\frac{\partial T}{\partial t}+u\frac{\partial T}{\partial x}+v\frac{\partial T}{\partial y}=\alpha_{nf}\left(\frac{\partial^2 T}{\partial x^2}+\frac{\partial^2 T}{\partial y^2}\right)+\frac{(\rho c)_p}{(\rho c)_{nf}}(D_B)_{nf}\left(\frac{\partial T}{\partial x}\frac{\partial C}{\partial x}+\frac{\partial T}{\partial y}\frac{\partial C}{\partial y}\right)+\frac{(\rho c)_p}{(\rho c)_{nf}}\frac{(D_T)_{nf}}{T_m}\left(\left(\frac{\partial T}{\partial x}\right)^2+\left(\frac{\partial T}{\partial y}\right)^2\right) \quad (4)$$

$$\frac{\partial C}{\partial t}+u\frac{\partial C}{\partial x}+v\frac{\partial C}{\partial y}=(D_B)_{nf}\left(\frac{\partial^2 C}{\partial x^2}+\frac{\partial^2 C}{\partial y^2}\right)+\frac{(D_T)_{nf}}{T_m}\left(\frac{\partial^2 T}{\partial x^2}+\frac{\partial^2 T}{\partial y^2}\right) \quad (5)$$

Where u and v denote the components of velocity in x and y direction correspondingly, $\upsilon_{nf}=\left(\mu_{nf}/\rho_{nf}\right)$denotesthe operational nanoliquids' kinematic viscosity, μ_{nf} denotes the nanoliquids' dynamic viscosity, ρ_{nf} represents the nanoliquids' density, T denotes temperature, T_m denotes mean temperature, C denotes nanoparticles concentration, $,p^*$ denotes pressure,σ_{nf} denotes nanoliquids' electrical conductivity, $B_o$denotes uniform magnetic field strength, $\alpha_{nf}=((k_{nf})/(\rho c_p)_{nf})$ denotes nanoliquids' thermal diffusivity, k_{nf}denotes fluid's thermal conductivity, $(\rho c_p)_{nf}$ denotes nanoliquids' functional heat capacity, $(\rho c)_p$ denotes nanoparticles' heat capacity, $(D_B)_{nf}$ denotes Brownian diffusion, $(D_T)_{nf}$ denotes theromphoretic diffusion coefficient, defined as (Ashwinkumar, 2018)(Tasawar Hayat *et al.*, 2016):

$$\rho_{nf}=(1-\xi)\rho_f+\xi\rho_s\ ,$$
$$\mu_{nf}=\frac{\mu_f}{(1-\xi)^{2.5}}$$
$$(\rho C_p)_{nf}=(1-\xi)(\rho C_p)_f+\xi(\rho C_p)_s$$
$$\alpha_{nf}=\frac{k_{nf}}{(\rho C_p)_{nf}},$$
$$\frac{k_{nf}}{k_f}=\left\{\frac{(k_s+(l-1)k_f)-(l-1)\xi(k_f-k_s)}{(k_s+(l-1)k_f)+\xi(k_f-k_s)}\right\},$$
$$\sigma_{nf}=\left(1+\frac{3.\left(\frac{\sigma_s}{\sigma_f}-1\right)\xi}{\left(\frac{\sigma_s}{\sigma_f}+2\right)-\left(\frac{\sigma_s}{\sigma_f}-1\right)\xi}\right),$$
$$(D_B)_{nf}=(1-\xi)(D_B)_f;(D_T)_{nf}=(1-\xi)(D_T)_f$$

Where ξ represents the nanoliquid's solid volume fraction, ρ_f represents base fluid's density, ρ_s represents the nanoparticle's density, μ_f represents base fluid's dynamic viscosity, $(\rho C_p)_f$ represents base fluid's heat capacity, $(\rho C_p)_s$represents nanoparticle's heat capacity, k_f represents base fluid's thermal conductivity and k_s represents nanoparticle's thermal conductivity.

$$u=U_o(x)=\frac{ax}{(1-\gamma t)},v=-\frac{v_0}{(1-\gamma t)}$$
$$T=T_o,C=C_o\ \ at\ \ y=0,$$
$$u=0,v=V_h=\frac{dh}{dt}=-\frac{\gamma}{2}\sqrt{\frac{\nu_f}{a(1-\gamma t)}}$$
$$T=T_o+\frac{T_o}{(1-\gamma t)},C=C_o+\frac{C_o}{(1-\gamma t)}\ \text{as}\ y=h(t) \quad (6)$$

Where a represents the lower plate's rate of stretching, $(V_o>0)$ denotes suction and $(V_o<0)$ denotes the velocity of injection/blowing, $T_o$and C_o represent the temperature and concentration of nanoparticles, respectively, at the lower wall. In periphery conditions (6), $U_o(x)=ax/(1-\gamma t)$ at $y=0$ suggest that the extensible (lower) plate linearly varies according to the distance variation from the origin. This supposition is accurate in many procedures including the procedure of extrusion wherein material attributes especially the extruded sheet elasticity that is pulled out using a steady force.
The transformations can be defined as:

$$u=U_oF'(\eta),v=-\sqrt{a\nu/(1-\gamma t)}\,F(\eta),,T=T_o+\frac{T_o}{(1-\gamma t)}\theta(\eta),C=C_o+\frac{C_o}{(1-\gamma t)}\phi(\eta)$$
$$\eta=y/h(t) \quad (7)$$

Discarding pressure gradient from Equations (2) and (3) and by using Equation (7) in the Equations (2) - (6), we have

$$F_{\eta\eta\eta\eta}+FF_{\eta\eta\eta}-F_\eta F_{\eta\eta}-\frac{S_q}{2}\left(3F_{\eta\eta}+\eta F_{\eta\eta\eta}\right)-\left(\frac{1}{1-\xi+\xi\left(\frac{\rho_s}{\rho_f}\right)}\right)(A_1)M^2F_{\eta\eta}=0 \quad (8)$$

$$\theta_{\eta\eta} + \Pr\left(\frac{k_f}{k_{nf}}\right)\left(\frac{1-\xi+\xi\left(\frac{Cp_s}{Cp_f}\right)}{(1-\xi)^{2.5}}\right)\left(F\theta_\eta - \frac{S_q}{2}\left(2\theta + \eta\theta_\eta\right) + (A_2)N_b\theta_\eta\phi_\eta + (A_2)N_t\theta_\eta^2\right) = 0 \quad (9)$$

$$\phi_{\eta\eta} + Le.\Pr\left(\frac{1-\xi+\xi\left(\frac{Cp_s}{Cp_f}\right)}{(1-\xi)^{3.5}}\right)\left(\frac{(1-\xi)^{-1}}{1-\xi+\xi\left(\frac{\rho_s.Cp_s}{\rho_f.Cp_f}\right)}\right)\left(F\phi_\eta - \frac{S_q}{2}\left(2\theta + \eta\phi_\eta\right)\right) + \frac{N_t}{N_b}\theta_{\eta\eta} = 0 \quad (10)$$

$$F = S, F' = 1, \theta = 0, \phi = 0 \text{ at} \eta = 0 \quad (11)$$

$$F = \frac{S_q}{2}, F' = 0, \theta = 1, \phi = 1 \text{ at} \eta = 1 \quad (12)$$

whereS_q represents squeezing parameter, M represents magnetic parameter, S represents blowing/suction parameter, Pr represents Prandtl number, Le represents Lewis number, N_b represents Brownian motion parameter and N_t represents thermophoresis parameter. These parameters are defined by

$$\mathrm{S_q} = \frac{\gamma}{a}, \mathrm{M^2} = \frac{\sigma \mathrm{B_o^2}}{\rho_f a}, \mathrm{S} = \frac{\mathrm{v_0}}{\mathrm{ah(t)}}, \mathrm{Pr} = \frac{\nu_f}{\mathrm{a_f}},$$
$$\mathrm{Le} = \frac{\mathrm{a_f}}{(\mathrm{D_B})_f}, \mathrm{N_b} = \frac{(\rho c)_p (\mathrm{D_B})_f (\mathrm{C_o})}{(\rho c)_f \nu_{f(1-\gamma t)}}$$
$$N_t = \frac{(\rho c)_p D_T (T_o)}{(\rho c)_f \nu_f T_m (1-\gamma t)} \quad (13)$$
$$A_1 = \left(1 + \frac{3.\left(\frac{\sigma_s}{\sigma_f} - 1\right)\xi}{\left(\frac{\sigma_s}{\sigma_f} + 2\right) - \left(\frac{\sigma_s}{\sigma_f} - 1\right)\xi}\right),$$
$$A_2 = \left(\frac{(1-\xi)^{3.5}\left(1-\xi+\xi\left(\frac{\rho_s}{\rho_f}\right)\right)}{1-\xi+\xi\left(\frac{\rho_s.Cp_s}{\rho_f.Cp_f}\right)}\right),$$
$$A_3 = \sqrt{(1-\xi)^{2.5}\left(1-\xi+\xi\left(\frac{\rho_s}{\rho_f}\right)\right)}$$

The coefficient of skin friction in dimensionless scale is given by

$$C_{fx} = \frac{(\tau_{wx})_{y=0}}{\rho_{nf} U_w^2} = \frac{\mu_{nf}\left(\frac{\partial u}{\partial y} + \frac{\partial v}{\partial x}\right)_{y=0}}{\rho_{nf} U_w^2} \quad (14)$$

The coefficient of skin friction in dimensionless scale is given by

$$Re_x^{1/2} C_{fx} = A_3 f''(0) \quad (15)$$

The local Nusselt number Nu_x and the local Sherwood number Sh_x are given as follows:

$$Nu_x = -\frac{x}{(T_w - T_o)}\left(\frac{\partial T}{\partial y}\right)_{y=0} = -\frac{1}{A_3}(Re_x)^{1/2}\theta'(0) \quad (16)$$

$$Sh_x = -\frac{x}{(C_w - C_o)}\left(\frac{\partial C}{\partial y}\right)_{y=0} = -\frac{1}{A_3}(Re_x)^{1/2}\emptyset'(0) \quad (17)$$

Where $Re_x = U_o x/\nu$ signifies the local Reynolds number (Ghadikolaei, Hosseinzadeh and Ganji, 2018), (S Ahmad *et al.*, 2018) (Farooq *et al.*, 2019).

3. NUMERICAL APPROACH AND VALIDATION

A series of non-similar eqns. (8) - (10) are nonlinear by nature and have no rational solution; therefore, a numerical handling would be more suitable. These series of ODE (ordinary differential equations) along with the periphery conditions (11, 12) are statistically solved by using 4th-5th order Runge-Kutta-Fehlberg method through Maple.

The Runge - Kutta - Fehlberg technique (represented by RKF45), (Lu *et al.*, 2017), (Ghadikolaei, Hosseinzadeh and Ganji, 2018) (S Ahmad *et al.*, 2018) is a significant technique used to solve this problem. There is a process in it that is used to determine whether the step size h used is appropriate. At every step, 2 separate approximations are made and evaluated to gain the solution. If both the approximations are near the solution, then they are accepted. If the 2 approximations do not converge with a particular accuracy, then the size of step is decreased. If the approximations are in agreement to more significant digits than what is required, there is an increase in the step size. Every step necessitates the use of 6 values as given below:

$$K_0 = f(x_n, y_n)h,$$
$$K_1 = f\left(x_n + \frac{1}{4}h, y_n + \frac{1}{4}K_0\right)h,$$
$$K_2 = f\left(x_n + \frac{3}{8}h, y_n + \frac{3}{32}K_0 + \frac{9}{32}K_1\right)h,$$
$$K_3 = f\left(x_n + \frac{12}{13}h, y_n + \frac{1932}{2197}K_0 - \frac{7200}{2197}K_1 + \frac{7296}{2197}K_2\right)h,$$
$$K_4 = f\left(x_n + h, y_n + \frac{439}{216}K_0 - 8K_1 + \frac{3680}{513}K_2 - \frac{845}{4104}K_3\right)h$$
$$K_5 = f\left(x_n + \frac{1}{2}h, y_n - \frac{8}{27}K_0 + 2K_1 - \frac{3544}{2565}K_2 + \frac{1859}{4104}K_3 - \frac{11}{40}K_4\right)h \quad (18)$$

Further, an approximation is made to the I.V.P. solution by using a Runge-Kutta technique of order 4:

$$y_{n+1} = y_n + \frac{25}{216}K_0 + \frac{1408}{2565}K_2 + \frac{2197}{4104}K_3 - \frac{1}{5}K_4 \quad (19)$$

Where the 4 function values *f*1, *f*3, *f*4, and *f*5 are employed. Observe that *f*2 is not employed in above formula (21). A more precise value is determined for the solution by using a Runge-Kutta technique of order 5:

$$\mathrm{z_{n+1}} = \mathrm{z_n} + \frac{16}{135}\mathrm{K_0} + \frac{6656}{12825}\mathrm{K_2} + \frac{28561}{56430}\mathrm{K_3} - \frac{9}{50}\mathrm{K_4} + \frac{2}{55}\mathrm{K_5} \quad (20)$$

The approximate error can be computed by deducting the two acquired values of y and z. The calculation of new step size can be done by

$$h_{new} = h_{old}\left[\frac{\epsilon h_{old}}{|z_{n+1}-y_{n+1}|}\right]^{1/4} \quad (21)$$

This Maple method is verified to be accurate and precise and it has been employed effectively to solve a broad range of nonlinear problems in the phenomena of transport particularly for heat transfer and flow issues. In this research, we have fixed the comparative error tolerance to10^{-8}.

We transform equations (8) - (10) into a first order equation system by writing:

$$\eta = y_1; f = y_2; f' = y_3; f'' = y_4; f''' = y_5; \theta = y_6; \theta' = y_7; \phi = y_8; \emptyset' = y_9 \quad (22)$$

$$\begin{bmatrix} y_1' \\ y_2' \\ y_3' \\ y_4' \\ y_5' \\ y_6' \\ y_7' \\ y_8' \\ y_9' \end{bmatrix} = \begin{bmatrix} 1 \\ y_3 \\ y_4 \\ y_5 \\ \left(\begin{matrix} -FF_{\eta\eta\eta} + F_\eta F_{\eta\eta} + \frac{S_q}{2}\left(3F_{\eta\eta} + \eta F_{\eta\eta\eta}\right) \\ +\left(\frac{1}{1-\xi+\xi\left(\frac{\rho_s}{\rho_f}\right)}\right)(A_1)M^2F_{\eta\eta} \end{matrix}\right) \\ y_7 \\ -\Pr\left(\frac{k_f}{k_{nf}}\right)\left(\frac{1-\xi+\xi\left(\frac{Cp_s}{Cp_f}\right)}{(1-\xi)^{2.5}}\right)\left(\begin{matrix} F\theta_\eta - \frac{S_q}{2}(2\theta + \eta\theta_\eta) + \\ (A_2)N_b\theta_\eta\phi_\eta + (A_2)N_t\theta_\eta^2 \end{matrix}\right) \\ y_9 \\ -Le.\Pr\left(\frac{1-\xi+\xi\left(\frac{Cp_s}{Cp_f}\right)}{(1-\xi)^{3.5}}\right)\left(\frac{(1-\xi)^{-1}}{1-\xi+\xi\left(\frac{\rho_s.Cp_s}{\rho_f.Cp_f}\right)}\right)\left(\begin{matrix} F\phi_\eta - \\ \frac{S_q}{2}(2\theta + \eta\phi_\eta) \end{matrix}\right) + \frac{N_t}{N_b}\theta_{\eta\eta} \end{bmatrix} \quad (23)$$

With initial conditions given below:

$$\begin{bmatrix} y_1(0) \\ y_2(0) \\ y_3(0) \\ y_4(0) \\ y_5(0) \\ y_6(0) \\ y_7(0) \\ y_8(0) \\ y_9(0) \end{bmatrix} = \begin{bmatrix} 0 \\ S \\ 1 \\ \chi_1 \\ \chi_2 \\ 0 \\ \chi_3 \\ 0 \\ \chi_4 \end{bmatrix} \quad (24)$$

Where, $[\chi_1, \chi_2, \chi_3, \chi_4] = [f''(\eta), f'''(\eta), \theta'(\eta), \phi'(\eta)]$, S denotes suction parameter. The method Runge-Kutta-Fehlberg was used to statistically integrate the 1st order system with 4th-5th order system by allotting suitable values to $\chi_1, \chi_2, \chi_3, \chi_4$ for iterative approximation of these quantities. The entire procedure is reiterated for different η_{max}; say - $\eta = 1$ until steady solutions are obtained exponentially inclined to free flow conditions by comparing them with MAPLE 18.

3.1 VALIDATION PROBLEM

With the aim to confirm the present statistical technique, the numerical outcomes are achieved for $f''(0)$, for different magnetic and suction parameter values. The outcomes of the comparisons are shown in Table-1 and are found to be accurate. The results of development of the squeezing 2D heat transfer and flow using nanoliquidare examined for various values of Brownian motion, injection/suction parameter, squeezing parameter, magnetic parameter, fraction of nanoparticle volume, Lewis number and thermophoresis parameter. In the next portion, the outcomes are discussed thoroughly using tables and plotted graphs.

4. RESULTS AND DISCUSSIONS

This section has been organised to study the impact of different pertinent parameters that include boiling/suction parameter S (only suction is studied in this research), squeezing flow parameter S_q, thermophoresis N_t, Brownian motion N_b, magnetic parameter M, nanoparticle volume fraction ξ and Lewis number Le on the profiles of temperature $\theta(\eta)$, velocity $F'(\eta)$, temperature, and nanoparticle concentration $\phi(\eta)$. Moreover, we examined the important quantities like coefficient of skin friction, the local Sherwood and Nusselt numbers which are showed as tables and graphs. Different kinds of base fluids are taken into account, which are ethylene glycol and water having 203.63 and 6.82 of Prandtl number, in order; as well as nanoparticle which is oxide aluminium(Al_2O_3) Table-2. The range of the fraction of the nanoparticle volume is assumed as $0.05 \leq \xi \leq 0.2$.

Figure-2 shows the velocity field magnetic effect in case of suction and it suggests that for a high M value,

the range of the velocity is reduced for $0 \leq \eta \leq 0.4$ and it is amplified when $0.4 \leq \eta \leq 1.0$.

When we raise M physically, there is a decrease in the velocity and it is also same in case of velocity gradient because the same rate of mass flow is enforced so as to fulfil the constraint of mass conservation. In flow of MHD, we suppose that the nanoliquid velocity decrease in the area of the walls will be equalised by a rise in the velocity of the nanoliquid around the central areas causing a cross flow activity

Table-1. Comparative of $f''(0)$ on lower surface for different values of S and M parameter when $S_q = K = 0$.

Parameter		**(Hayat, Sajjad, *et al.*, 2017)**		**Present work**
S	M	Numerical	HAM	(RKF45)
0.5	0.0	-7.411153	-7.411153	-7.41115251
	1.0	-7.591618	-7.591618	-7.59161764
	2.0	-8.110334	-8.110334	-8.11033418
	3.0	-8.910096	-8.910096	-8.91009560
0.0	2.0	-4.587891	-4.587891	-4.58789111
0.3		-6.665662	-6.665662	-6.66566201
0.6		-8.851444	-8.851444	-8.85144420
1.0		-11.94858	-11.94858	-11.9485841

Table-2. Thermos-physical properties of water, ethylene glycol and nanoparticle (Esfahani and Bordbar, 2011).

	$\rho(kg/m^3)$	$C_p(JkgK)$	$K\ (W/mk)$	$\sigma\ (\Omega^{-1}m^{-1})$	**Prandtl number**
Pure water	997.1	4179	0.613	5.5	6.82
Ethylene glycol	1115	2430	0.253	1.07	203.63
Al_2O_3	3970	765	40	16.7	-

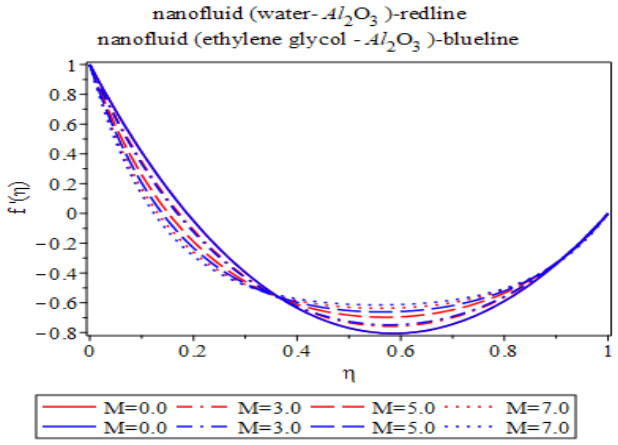

Figure-2. Effect of different magnetic field on velocity parameter.

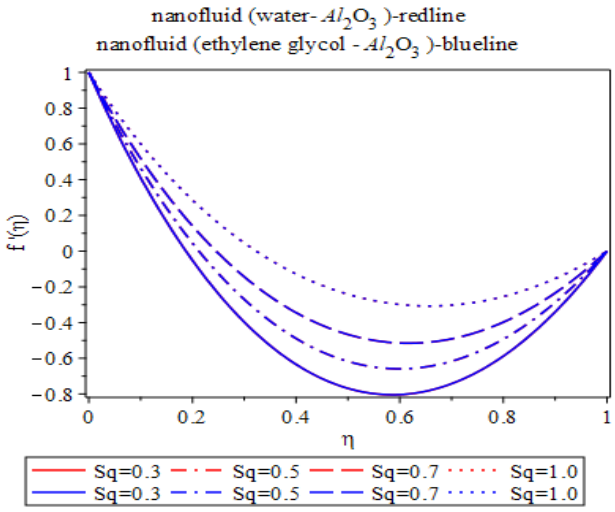

Figure-3(a). Effect of different squeezed flow on velocity parameter.

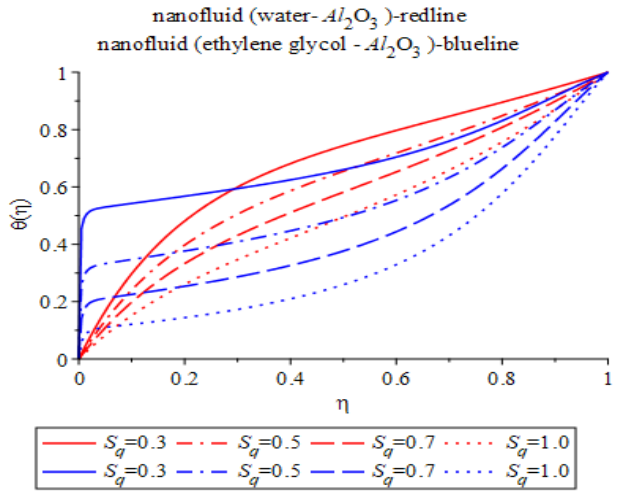

Figure-3(b). Effect of different squeezed flow on temperature parameter.

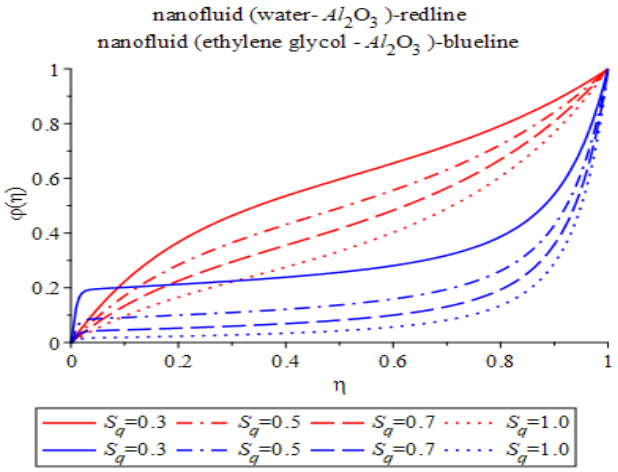

Figure-3(c). Effect of different squeezed flow on nanoparticle concentration parameter.

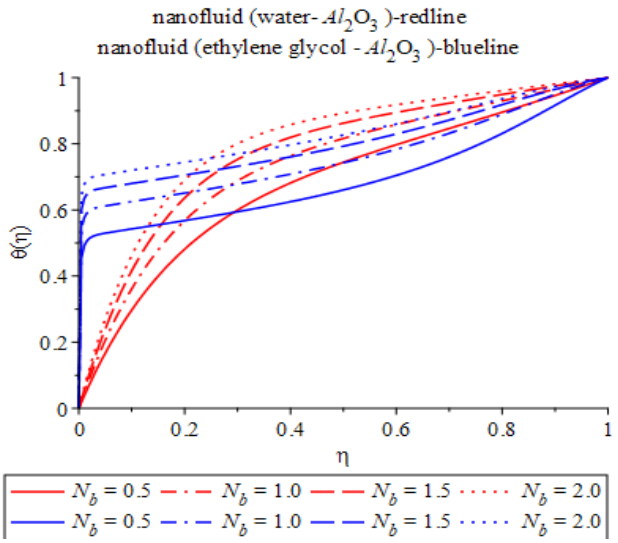

Figure-4. Effect of different Brownian motion on temperature parameter.

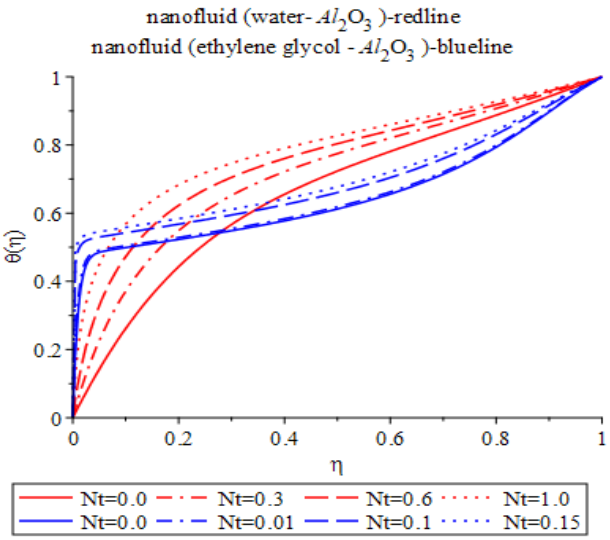

Figure-5. Effect of different thermophoresis on temperature profile.

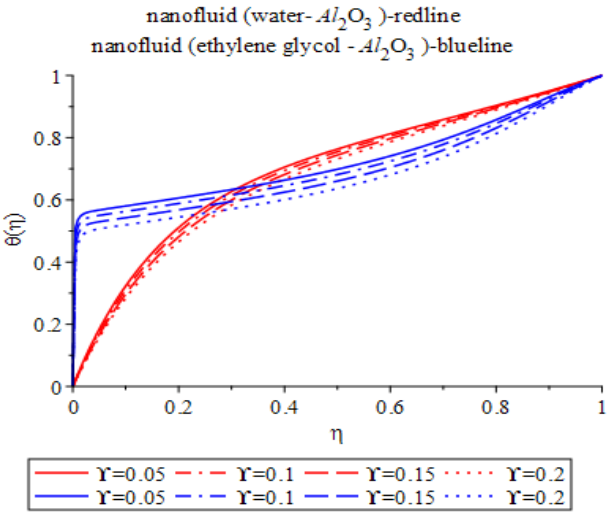

Figure-6. Effect of different nanoparticle volume fraction parameter on temperature.

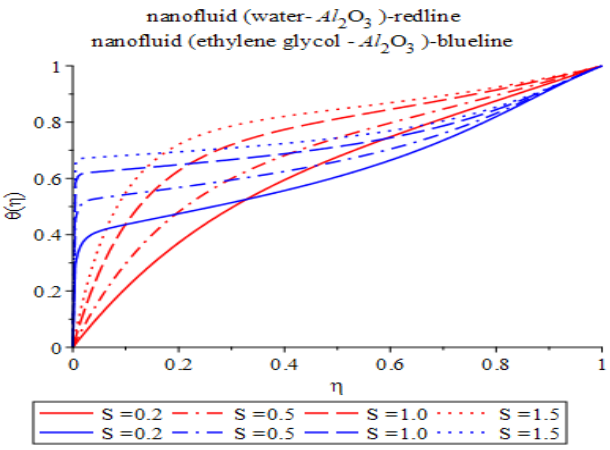

Figure-7(a). Different suction parameter on temperature profile.

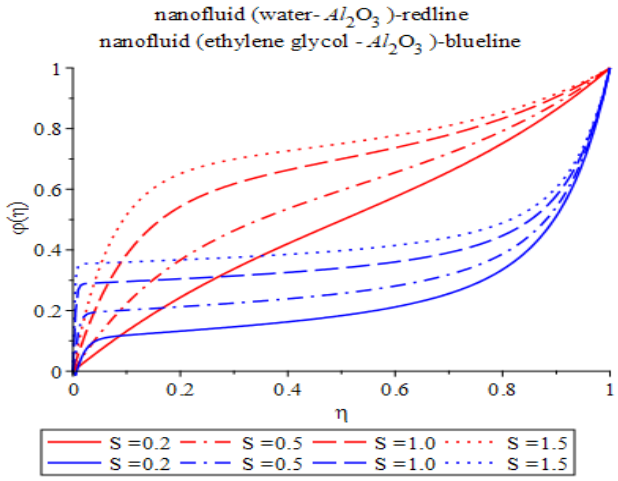

Figure-7(b). Different suction parameter on nanoparticle concentration profile.

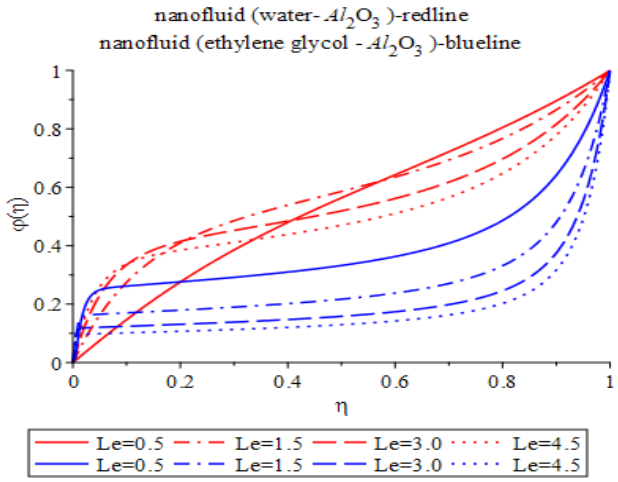

Figure-8. Effect of different Lewis number on nanoparticle concentration parameter.

The impact of S_q (squeezing effect) is demonstrated in Figures 3(a), (b), and (c). In Figure 3 (a), it can be observed that the range of velocity $F'(\eta)$ is decreased near the porous wall in the lower region where the effect of suction is prominent. Conversely, the wall in the upper area shifts in the way of stretching the porous wall such that the nanoliquids are enhanced by the pressure flow in common. Subsequently, the stream with the field of velocity around the upper wall region increases to preserve the constraint of mass conservation. The effects of temperature on the squeezed nanoliquidsare demonstrated in Figure-3b, which are reduced for bigger value of ethylene glycol and water squeezing parameter. Squeezing parameter impact $S_q$on the concentration field of nanoparticle $\phi(\eta)$ in the case of suction is illustrated in Figure-3(c). The concentration of nanoparticles in the field of nanoliquids is decreased at the time of increase in the squeezing parameter value. The effect of the parameter of Brownian motion N_b on the profile of temperature $\theta(\eta)$is illustrated in figure 4. Here, the profile of temperature improves as per the Brownian motion parameter increase. A Brownian motion parameter increase signifies a higher coefficient of Brownian diffusion, and it confirms a stronger profile of temperature.

Figure-5 shows that the profile of temperature $\theta(\eta)$ is improved with the rise in thermophoresis factor N_t. A rise in this parameter $0.0 \leq N_t \leq 0.15$ for ethylene glycol and $0.0 \leq N_t \leq 1.0$ for water makes the thermophoresis force stronger, which in turn causes a greater temperature profile.

The impact of the fraction of nanoparticle volume on the profile of temperature is shown in Figure-6. In the figure, it can be seen that there is a decrease in the temperature with the increase in the fraction of the nanoparticle volume. Figures 7(a) and 7(b) show the suction parameter S in nanoparticle concentration and temperature profile. A rise in the suction parameter caused a rise in the temperature and the effect of nanoparticle concentration.

The variation in the concentration field of nanoparticle $\phi(\eta)$ for various Lewis number Le values is shown in Figure-8. The concentration field of nanoparticle is decreased when the Lewis number values are increased. Lewis number Le varies inversely as the coefficient of Brownian diffusion. The coefficient of Brownian diffusion is lower for greater Lewis number. This lower value of coefficient of Brownian diffusion causes weakening of the concentration field of the nanoparticle.

Table-3 and Table-4 displays that magnetic parameter M, suction parameter S and fraction of nanoparticle volume parameter ξ are predominant factors affecting the skin friction rate for ethylene glycol and water. Also the squeezing flow, magnetic field parameter and fraction of nanoparticle volume improved the transfer of heat attribute of nanoliquids as displayed in Table-3 and Table-4 in the Nusselt number column for ethylene glycol and water. As far as the mass transfer rate is concerned, we can observe that the parameters squeezing flow and magnetic field are positively affected for water, while in the case of ethylene glycol, the parameters Brownian motion and suction are increased.

5. CONCLUSIONS

A two-dimensional Magneto-hydrodynamic squeezing flow is analysed numerically in this study. In the presence of nanoliquids (water/ethylene glycol-Al_2O_3), the flow is examined over a porous stretching surface. The major findings of the study are as follows:

- There is an increase in temperature $\theta(\eta)$with an increase in values of $N_t$and N_b.
- The velocity field improves with an increase in the squeezing parameter S_q. On the other hand, an increase in the value of squeezing parameter S_q reduces the nanoparticle concentration profiles and the temperature. A rise in the Lewis number Le results in a decline in the nanoparticle concentration field $\phi(\eta)$

In Tables 3 and 4:

- The heat transfer of nanoliquids improved with an enhancement of the nanoparticle volume fraction, the squeezing flow and the magnetic field parameter.
- The nanoparticle volume fraction parameter ξ, the suction parameter S, and the magnetic parameter M play a dominant role in deciding the rate of skin friction for ethylene glycol and water.
- The suction parameter and the Brownian motion promote the rate of mass transfer of ethylene glycol.
- The squeezing flow parameter and the magnetic field have a positive effect on the rate of mass transfer of water.

Table-3. The rate of skin friction, rate of heat and mass transfer of lower wall for nanoliqid($water - Al_2O_3$) with different value of S, M, S_q, ξ, N_b, Le.

$water - Al_2O_3$								
S	**M**	S_q	ξ	N_b	Le	$C_{fx}(Re_x)^{1/2}$	$Nu_x(Re_x)^{-1/2}$	$Sh_x(Re_x)^{-1/2}$
0.2	0.5	0.3	0.15	0.5	1.0	-4.54569114	-2.37340433	-1.42464687
0.5						-6.57368588	-3.76558324	-2.74392134
1.0						-10.2177912	-6.64255566	-5.84883250
1.5						-14.2330000	-9.85461817	-9.49584610
0.5	0.0	0.3	0.15	0.5	1.0	-6.53950376	-3.76739682	-2.74575983
	3.0					-7.67985950	-3.71045629	-2.68824117
	5.0					-9.37319824	-3.63835095	-2.61604728
	7.0					-11.4334682	-3.56734616	-2.54570126
0.5	0.5	0.3	0.15	0.5	1.0	-6.57368588	-3.76558324	-2.74392134
		0.5				-5.98132016	-2.98514312	-2.09347680
		0.7				-5.38180808	-2.42005620	-1.63988535
		1.0				-4.46927737	-1.82330907	-1.17843642
0.5	0.5	0.15	0.05	0.5	1.0	-6.57779184	-4.24533492	-1.94945006
			0.1			-6.57545916	-3.99988693	-2.31174629
			0.15			-6.57368588	-3.76558324	-2.74392134
			0.2			-6.57232019	-3.54502755	-3.25954158
0.5	0.5	0.3	0.15	0.5	1.0	-6.57368588	-3.76558324	-2.74392134
				1.0		-6.57368588	-4.70434874	-2.95880036
				1.5		-6.57368588	-5.55199449	-3.04123890
				2.0		-6.57368588	-6.31698158	-3.08853646
0.5	0.5	0.3	0.15	0.5	0.5	-6.57368589	-3.63474234	-1.53294397
					1.5	-6.57368588	-3.82037456	-3.88697859
					3.0	-6.57368588	-3.81815007	-6.69293137
					4.5	-6.57368588	-3.76932884	-8.97372982

Table-4. The rate of skin friction, rate of heat and mass transfer of lower wall for nanoliqid($ethylene\ glycol - Al_2O_3$)with different value of S, M, S_q, ξ, N_b, Le .

$ethyleneglycol - Al_2O_3$								
S	M	S_q	ξ	N_b	Le	$C_{fx}(Re_x)^{1/2}$	$Nu_x(Re_x)^{-1/2}$	$Sh_x(Re_x)^{-1/2}$
0.2	0.5	0.3	0.15	0.5	1.0	-4.55265710	-924.18407568	177.12482841
0.5						-6.58218916	-9997.99133381	1968.61241939
1.0						-10.2286746	-73860.62352209	14680.47833360
1.5						-14.2459493	-229132.7704693	45658.28296872
0.5	0.0	0.3	0.15	0.5	1.0	-6.53950376	-10027.80572946	1974.54587434
	3.0					-7.93965336	-9191.16151265	1808.04031151
	5.0					-9.95291189	-8209.25785799	1612.57768208
	7.0					-12.3413839	-7787.08433828	1528.48765083
0.5	0.5	0.3	0.15	0.5	1.0	-6.58218916	-9997.99133381	1968.61241939
		0.5				-5.98927314	-610.32955443	108.39843843
		0.7				-5.38921659	-108.05967395	14.88794710
		1.0				-4.47587986	-21.76273480	1.70458569
0.5	0.5	0.15	0.05	0.5	1.0	-6.58099267	-145194.9701074	29013.0856802
			0.1			-6.58143138	-36146.89757985	7201.11125028
			0.15			-6.58218916	-9997.991345496	1968.61242173
			0.2			-6.58323953	-3164.672337663	598.798521422
0.5	0.5	0.3	0.15	0.5	1.0	-6.58218916	-9997.99133381	1968.61241939
				1.0		-6.58218916	-33190.52326222	3288.35278021
				1.5		-6.58218916	-75614.33171348	5010.32371362
				2.0		-6.58218916	-139506.7876715	6944.7353638
0.5	0.5	0.3	0.15	0.5	0.5	-6.58218916	-13372.13435915	2653.8860870
					1.5	-6.58218916	-8333.64831784	1627.7498298
					3.0	-6.58218916	-6054.74892700	1154.5305601
					4.5	-6.58218916	-5036.01680233	938.17737057

REFERENCE

Ahmad S. *et al.* 2018. Double stratification effects in chemically reactive squeezed Sutterby fluid flow with thermal radiation and mixed convection. Results in physics. Elsevier. 8, pp. 1250-1259.

Ahmad S. et al. 2018. Entropy generation optimization and unsteady squeezing flow of viscous fluid with five different shapes of nanoparticles. Colloids and Surfaces A: Physicochemical and Engineering Aspects. Elsevier.

Ashwinkumar G. P. 2018. Effect of radiation absorption and buoyancy force on the MHD mixed convection flow of Casson nanofluid embedded with Al50Cu50 alloy nanoparticles. Multidiscipline Modeling in Materials and Structures. Emerald Publishing Limited. 14(5): 1082-1100.

Chol S. U. S. and Estman J. A. 1995. Enhancing thermal conductivity of fluids with nanoparticles. ASME-Publications-Fed. ASME. 231, pp. 99-106.

Dib A., Haiahem A. and Bou-Said B. 2015. Approximate analytical solution of squeezing unsteady nanofluid flow. Powder Technology. Elsevier. 269, pp. 193-199.

Dogonchi A. S., Alizadeh M. and Ganji D. D. 2017. Investigation of MHD Go-water nanofluid flow and heat transfer in a porous channel in the presence of thermal radiation effect. Advanced Powder Technology. Elsevier. 28(7): 1815-1825.

Domairry G. and Hatami M. 2014. Squeezing Cu-water nanofluid flow analysis between parallel plates by DTM-Padé Method. Journal of Molecular Liquids. Elsevier. 193, pp. 37-44.

Esfahani J. A. and Bordbar V. 2011. Double diffusive natural convection heat transfer enhancement in a square enclosure using nanofluids. Journal of Nanotechnology in Engineering and Medicine. American Society of Mechanical Engineers. 2(2): 21002.

Fang M., Gilbert R. P. and Liu X.-G. 2010. A squeeze flow problem with a Navier slip condition. Mathematical and Computer Modelling. Elsevier. 52(1-2): 268-277.

Farooq M. et al. 2019. Melting heat transfer in squeezed nanofluid flow through Darcy Forchheimer medium. Journal of Heat Transfer. American Society of Mechanical Engineers. 141(1): 12402.

Freidoonimehr N. et al. 2017. Analytical approximation of heat and mass transfer in MHD non-Newtonian nanofluid flow over a stretching sheet with convective surface boundary conditions. International Journal of Biomathematics. World Scientific. 10(01): 1750008.

Freidoonimehr N., Rostami B. and Rashidi M. M. 2015. Predictor homotopy analysis method for nanofluid flow through expanding or contracting gaps with permeable walls. International Journal of Biomathematics. World Scientific. 8(04): 1550050.

Ghadikolaei S. S., Hosseinzadeh K. and Ganji D. D. 2018. Investigation on three dimensional squeezing flow of mixture base fluid (ethylene glycol-water) suspended by hybrid nanoparticle (Fe3O4-Ag) dependent on shape factor. Journal of Molecular Liquids. Elsevier. 262, pp. 376-388.

Gul A. et al. 2015. Heat transfer in MHD mixed convection flow of a ferrofluid along a vertical channel. PloS one. Public Library of Science. 10(11): e0141213.

Gupta A. K. and Ray S. S. 2015. Numerical treatment for investigation of squeezing unsteady nanofluid flow between two parallel plates', Powder Technology. Elsevier. 279, pp. 282-289.

Hatami M., Nouri R. and Ganji D. D. 2013. Forced convection analysis for MHD Al2O3-water nanofluid flow over a horizontal plate. Journal of Molecular Liquids. Elsevier. 187, pp. 294-301.

Hayat T., Yousaf A., et al. 2012. MHD squeezing flow of second-grade fluid between two parallel disks. International Journal for Numerical Methods in Fluids. Wiley Online Library. 69(2): 399-410.

Hayat T., Farooq M., et al. 2012. Mixed convection Falkner-Skan flow of a Maxwell fluid. Journal of Heat Transfer. American Society of Mechanical Engineers. 134(11): 114504.

Hayat T. et al. 2016. Effects of homogeneous - heterogeneous reactions in flow of magnetite-Fe3O4 nanoparticles by a rotating disk. Journal of Molecular Liquids. Elsevier. 216, pp. 845-855.

Hayat T. et al. 2016. On squeezing flow of nanofluid in the presence of magnetic field effects. Journal of Molecular Liquids. Elsevier. 213, pp. 179-185.

Hayat T., Khan M., et al. 2017. A useful model for squeezing flow of nanofluid. Journal of Molecular Liquids. Elsevier. 237, pp. 447-454.

Hayat T., Sajjad R., et al. 2017. On squeezed flow of couple stress nanofluid between two parallel plates. Results in physics. Elsevier. 7, pp. 553-561.

Idrees M. et al. 2010. Application of the optimal homotopy asymptotic method to squeezing flow. Computers & Mathematics with Applications. Elsevier. 59(12): 3858-3866.

Khan U., Ahmed N., Zaidi Z. A., et al. 2014. MHD squeezing flow between two infinite plates. Ain Shams Engineering Journal. Elsevier. 5(1): 187-192.

Khan U., Ahmed N., Khan S. I., et al. 2014. On unsteady two-dimensional and axisymmetric squeezing flow between parallel plates. Alexandria Engineering Journal. Elsevier. 53(2): 463-468.

Loganathan P., Nirmal Chand P. and Ganesan P. 2013. Radiation effects on an unsteady natural convective flow of a nanofluid past an infinite vertical plate. Nano. World Scientific. 8(01): 1350001.

Lu D. et al. 2017. A numerical treatment of radiative nanofluid 3D flow containing gyrotactic microorganism with anisotropic slip, binary chemical reaction and activation energy. Scientific reports. Nature Publishing Group. 7(1): 17008.

Madaki A. G. et al. 2018. Analytical and numerical solutions of squeezing unsteady Cu and TiO2-nanofluid flow in the presence of thermal radiation and heat generation/absorption. Alexandria Engineering Journal. Elsevier. 57(2): 1033-1040.

Mahanthesh B., Gireesha B. J. and Gorla R. S. R. 2016. Mixed convection squeezing three-dimensional flow in a rotating channel filled with nanofluid. International Journal of Numerical Methods for Heat & Fluid Flow. Emerald Group Publishing Limited. 26(5): 1460-1485.

Muhammad T. et al. 2017. Hydromagnetic unsteady squeezing flow of Jeffrey fluid between two parallel plates. Chinese Journal of Physics. Elsevier. 55(4): 1511-1522.

Petrov A. G. and Kharlamova I. S. 2014. The solutions of Navier-Stokes equations in squeezing flow between

parallel plates. European Journal of Mechanics-B/Fluids. Elsevier. 48, pp. 40-48.

Seyedi S. H., Saray B. N. and Ramazani A. 2018. On the multiscale simulation of squeezing nanofluid flow by a highprecision scheme. *Powder Technology*. Elsevier. 340, pp. 264-273.

Sheikholeslami M. *et al.* 2018. Numerical modeling for alumina nanofluid magnetohydrodynamic convective heat transfer in a permeable medium using Darcy law. International Journal of Heat and Mass Transfer. Elsevier. 127, pp. 614-622.

Sheikholeslami M., Abelman S. and Ganji D. D. 2014. Numerical simulation of MHD nanofluid flow and heat transfer considering viscous dissipation. International Journal of Heat and Mass Transfer. Elsevier. 79, pp. 212-222.

Sheikholeslami M. and Ganji D. D. 2013. Heat transfer of Cu-water nanofluid flow between parallel plates. Powder Technology. Elsevier. 235, pp. 873-879.

Sheikholeslami M., Ganji D. D. and Ashorynejad H. R. 2013. Investigation of squeezing unsteady nanofluid flow using ADM. Powder Technology. Elsevier. 239, pp. 259-265.

Sheikholeslami M., Hatami M. and Domairry G. 2015. Numerical simulation of two phase unsteady nanofluid flow and heat transfer between parallel plates in presence of time dependent magnetic field. Journal of the Taiwan Institute of Chemical Engineers. Elsevier. 46, pp. 43-50.

Sobamowo M. G., Jayesimi L. O. and Waheed M. A. 2018. Magnetohydrodynamic squeezing flow analysis of nanofluid under the effect of slip boundary conditions using variation of parameter method. Karbala International Journal of Modern Science. Elsevier. 4(1): 107-118.

Usman M. *et al.* 2018. Heat and fluid flow of water and ethylene-glycol based Cu-nanoparticles between two parallel squeezing porous disks: LSGM approach. International Journal of Heat and Mass Transfer. Elsevier. 123, pp. 888-895.

Zaimi K., Ishak A. and Pop I. 2014. Boundary layer flow and heat transfer over a nonlinearly permeable stretching/shrinking sheet in a nanofluid. Scientific Reports. Nature Publishing Group. 4, p. 4404.